Assessment of a CFD model for short-range plume dispersion: Applications to the Fusion Field Trial 2007 (FFT-07) diffusion experiment

Pramod Kumar, Sarvesh Kumar Singh, Pierre Ngae, Amir Ali Feiz, Grégory Turbelin

Assessment of a CFD model for short-range plume dispersion: Applications to the Fusion Field Trial 2007 (FFT-07) diffusion experiment

Pramod Kumar*, Sarvesh Kumar Singh, Pierre Ngae, Amir-Ali Feiz, Grégory Turbelin

LMEE, Université d'Evry Val-d'Essonne, 40 Rue Du Pelvoux, Courcouronnes 91020, France

Simulations of the short-range plume dispersion under different atmospheric conditions can provide essential information for the development of source reconstruction methodologies that allows to retrieve the location and intensity of an unknown hazardous pollutant source. This process required a comprehensive assessment of the atmospheric dispersion models with tracer diffusion experiments in various stability conditions. In this study, a comprehensive evaluation of a CFD model fluidyn-PANACHE is performed with the observations from available seven trials of single releases conducted in the Fusion Field Trail 2007 (FFT-07) tracer experiment. The CFD simulations are performed for each trial and it was observed that the CFD model fluidyn-PANACHE provides good agreement of the predicted concentrations with the observations in both stable and convective atmospheric conditions. A comprehensive analysis of the simulated results is performed by computing the statistical performance measures for the dispersion model evaluation. The CFD model predicts 65.4% of the overall concentration points within a factor of two to the observations. It was observed that the CFD model is predicting better in convective stability conditions in comparison to the trials conducted in stable stability. In convective conditions, 74.6% points were predicted within a factor of two to the observations which are higher than 59.3% concentration points predicted within a factor of two in the trials in stable atmospheric conditions.

1. Introduction

In case of an accidental or deliberated release of the air pollutants or harmful substances into the atmosphere, it is important to predict where, when and how seriously a released contaminant can affect a specific region. In these situations, the atmospheric dispersion of hazardous contaminants is the first concern for the exposure on surrounding environment and human health, emergency response and risk assessment. The dispersion of air pollutants in the atmosphere is a challenging problem due to the complex interaction of plume with turbulent eddies and complex nature of inhomogeneous sheared turbulence near a rough boundary, meteorological and stability conditions such as wind, temperature inversion and foggy atmosphere (Kumar and Sharan, 2010). Accurate modelling of the atmospheric dispersion of pollutants is also an essential step towards developing the source reconstruction process to retrieve the location and intensity of an unknown release in a specific region (Sharan et al., 2009; Kumar et al., 2015b, etc.).

Over the years, attempts have been made for accurate modelling dispersion of pollutants released from continuous point sources in diverse atmospheric conditions using various types of the dispersion models. Several types of dispersion models, e.g., conventional Gaussian plume models (Sharan et al., 1996; Cimorelli et al., 2005, etc.), dispersion models based on the analytical solutions of simplified form of the advection-diffusion equation (Vilhena et al., 2008; Moreira et al., 2009; Kumar and Sharan, 2010, etc.), Lagrangian dispersion models (Stohl et al., 2005; Stein et al., 2015, etc.), and hybrid plume dispersion models (HPDM) (Hanna and Paine, 1989), etc. have been frequently used for short-range plume dispersion in diverse atmospheric stability conditions. With rapid advances in computer resources and methods, Computational Fluid Dynamics (CFD) models provide accurate flow fields and pollutant dispersion modelling in diverse regions for various kind of release scenarios that includes the continuous or instantaneous releases from the point, area, volume, and other general sources (Liu and Wong, 2014; Kumar et al., 2015a; Kumar and Feiz, 2016, etc.). The dispersion in the diffusion models with Computational Fluid Dynamics can be model either in Eulerian or Lagrangian particle modelling framework (Zhang and Chen, 2007). However, it is essential to examine the real predictive capability of the CFD modelling approaches to apply it in emergency contexts of an accidental or deliberate hazardous release in diverse atmospheric conditions. For this purpose, a comprehensive evaluation of the CFD model is required with the concentration

* Corresponding author.
E-mail address: pramod.kumar@univ-evry.fr (P. Kumar).

observations from a tracer field experiment in different stability conditions.

In order to evaluate the CFD simulations for pollutant dispersion in diverse atmospheric conditions, completeness and reliability of an experimental data is a necessity. Recently, a comprehensive and highly instrumented tracer field experiment called FUsing Sensor Information from Observing Networks (FUSION) Field Trial-2007 (FFT-07) was conducted in September, 2007 at Dugway Proving Ground, Utah, USA for short-range dispersion (≈ 500 m) of the pollutant released from point sources (Storwold, 2007; Platt et al., 2008). The main objective of this tracer field experiment was a comparative investigation of the Source Term Estimation (STE) methodologies in different atmospheric and release scenarios (Platt et al., 2008). The problem of the STE has attracted attention for fast and accurate identification of the unknown accidental or deliberated releases from a finite set of the atmospheric concentration measurements acquired from a deployed monitoring network (Pudykiewicz, 1998; Bocquet, 2005; Sharan et al., 2009; Kumar et al., 2015b; Kumar et al., 2016, etc.). The STE algorithms are required to use data from networked chemical and biological (CB) and other (e.g., meteorological) sensors to (1) estimate the source characteristics (source location and magnitude), and (2) refine dispersion model predictions of downwind hazards (Storwold, 2007). The FFT-07 experiment was designed to fill a key STE validation data gap, the lack of high spatial and temporal resolution dispersion measurements for single and simultaneous multiple source releases. The FFT-07 tracer field experiment includes an extensive set of the meteorological, turbulence, and concentration measurements from single, multiple, continuous and instantaneous point releases in diverse atmospheric conditions. Recently, Singh and Sharan (2013) and Pandey and Sharan (2015) evaluated a Gaussian plume dispersion model respectively for single and multiple releases trials of the FFT-07 experiment in which multiple release refers to several releases at the same time from different positions. The FFT-07 dataset completeness and high quality make the experiment an exceptional candidate for the assessment of a CFD model for near-field plume dispersion in different atmospheric stability conditions. The FFT-07 experiment is required to validate, under real-world atmospheric conditions, for forward atmospheric dispersion and the STE algorithms under development to satisfy the requirements for source characterization and hazard prediction refinement.

In this study, a CFD model fluidyn-PANACHE is evaluated with the several available trials of the FFT-07 field experiment in different atmospheric conditions. The CFD model fluidyn-PANACHE is a self-contained fully 3-dimensional (3-D) fluid dynamics, commercial CFD code, designed to simulate accidental and industrial pollutant dispersion in diverse terrains, atmospheric and release scenarios. Three-dimensional numerical simulations for each selected FFT-07 trial were performed for near-field plume dispersion from a single point continuous release using the fluidyn-PANACHE. The dispersion characteristics of the released plume from the CFD simulations are analyzed both qualitatively and quantitatively following the various statistical performance measures for air dispersion model evaluation.

2. Fusion Field Trial 2007 (FFT-07) field experiment

In this study, we utilized a recently conducted short range (≈ 500 m) comprehensive tracer field experiment at the U.S. Army's Dugway Proving Ground (DPG), Utah in September, 2007 (Storwold, 2007; Platt et al., 2008). This highly instrumented tracer experiment is referred to as FUsing Sensor Information from Observing Networks (FUSION) Field Trial 2007 (FFT-07). Most of the existing dispersion datasets measured dosages (time-integrated concentrations), which makes it impossible to replicate the instantaneous concentrations that would have challenged Chemical and Biological (CB) detectors. Only those existing dispersion datasets with high temporal resolution (1 to 50 Hz sampling rate) concentration measurements can be used with

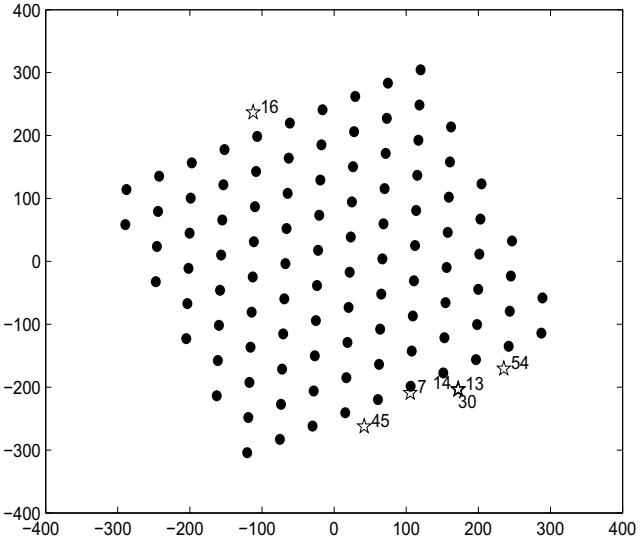

Fig. 1. Schematic layout of the FFT-07 geometry showing 100 sensor locations. The black filled circles denote the position of receptors. The stars denote the source locations of the selected trials - only one was operational in a given trial.

signal processing to simulate the responses of current and future CB detectors to real-world challenges. Consequently, the conceptual design for the FFT-07 was to fill the gaps in the real world data needed to validate current and future STE algorithms (Storwold, 2007). The STE methodologies developed or validated using the FFT-07 dataset can be a step towards to utilize/improve these techniques to estimate the sources in urban or other geometrically complex regions. The FFT-07 experiment provides high spatial and temporal resolution dispersion and meteorological measurements. It includes the concentration observations from various instantaneous, continuous, single as well as multiple point releases in various atmospheric stability conditions varying from neutral to stable, and unstable conditions.

The design concept of the FFT-07 was to collect data from an abundance of research-grade tracer, sensor, and meteorological instruments rather than employing an “optimal” placement strategy (Storwold, 2007). In this experiment, propylene (C_3H_6) was released at 2 m height above the ground surface and the concentrations were measured at 100 fast response digital Photo Ionization Detector (digiPID) sensors deployed in a rectangular staggered grid of area 475 m × 450 m in 10 rows and 10 columns (Fig. 1). The digiPID samplers were deployed at 2 m height above the ground surface and the position of tracer source was altered according to the ambient wind direction in each trial. The terrain of the experimental site was uniform and homogeneous consisting primarily of short grass interspersed with low shrubs with a height between about 0.25 m and 0.75 m with the momentum roughness length, $z_0 = 0.013 \pm 0.002$ m (Yee, 2012).

Extensive meteorological and turbulence measurements from many Portable Weather Instrumentation Data system (PWIDs) and ultrasonic anemometer/thermometer (sonic) and other instruments were acquired during this experiment. Three-dimensional sonic anemometers were mounted at five levels (2, 4, 8, 16, and 32 m) on three towers located at grid centre, 750 m north-northwest of grid centre, and 750 m south-southwest of grid centre. The sonic data from these three towers is processed to produce wind and turbulence statistics and surface fluxes of heat and momentum. In this study, the observations from seven FFT-07 trials 07, 13, 14, 16, 30, 45 and 45 in different atmospheric stability conditions are considered and utilized for the forward dispersion of tracer from a single point release. The atmospheric stability in each selected FFT-07 trial was categorized based on the sign of the Obukhov length (L) computed by the eddy covariance method from the sonic data measured at 4 m level of the centre tower. Other meteorological variables, e.g., wind speed, directions, and ambient air temperature, etc. are

also computed from the fast response data at 4 m level of the centre tower.

3. Description of the CFD model fluidyn-PANACHE

A CFD model fluidyn-PANACHE (Mazzoldi et al., 2008; Fluidyn-PANACHE, 2010; Kumar et al., 2015a) is utilized in this study for forward plume dispersion from a point release. The fluidyn-PANACHE solves the 3-dimensional (3-D) Reynolds Averaged Naiver-Stokes (RANS) fluid dynamics equations using finite volume numerical techniques. It includes the numerical solutions for both steady and unsteady forms of the RANS equations. In this study, steady RANS solution along with the full conservation equations governing the transport of species concentration, mass, heat transfer and energy for a mixture of ideal gases is utilized for the simulations of flow-field and atmospheric dispersion. In this CFD model, a linear eddy viscosity model of Ferziger and Peric (2002) is used to model the Reynolds stresses. A modified standard k-ϵ turbulence model that solves the transport equations for turbulent kinetic energy k and its dissipation rate ϵ, is used to compute the turbulent structure in domain. In this, the standard k-ϵ model was modified to include the effects of buoyancy and the stability condition of the atmosphere by means of Richardson number, a non-dimensional parameter characterizing the stability of the atmosphere in terms of temperature (Mazzoldi et al., 2008). The standard Eulerian advection-diffusion equation governing the transport and diffusion of air pollutants is solved to simulate dispersion in the FFT-07 tracer experiment. In the CFD model fluidyn-PANACHE, air is treated as compressible and the dispersion is introduced as a passive scalar. In simulations, the Schmidt number (Sc) is taken equal to 0.7.

4. Numerical setup and simulations

4.1. Computational setup and mesh

The study domain for numerical simulations comprises outer and inner domains of width × length of 2000 m × 2000 m and 1000 m × 1000 m, respectively. The inner (nested) domain comprises all the source, sensors and other instruments. To ensure a smoothly varying wind flow over the boundary of inner domain, outer domain boundary was kept away from the main test site consisting all the sensors and instruments and thus, the size of the outer computational domain was considered approximately twice of the inner domain. The heights of inner and outer domains were taken as 100 m and 200 m, respectively. The 3-D unstructured mesh is considered in both outer and inner domains. Mesh is more refined near to the locations of source, receptors and other positions of the instruments. These inner and outer domains discretized into 55 and 60 vertical levels, respectively. In both domains, lowest 39 vertical levels are set with a uniform 0.25 m grid spacing that formed the lowest 10 m of the vertical domains. Above the 10 m level, the vertical grid spacing are set to uniform 2 m (5 vertical levels between 10 m and 20 m), 5 m (4 levels between 20 m and 40 m), 10 m (6 levels between 40 m and 100 m), and, 20 m (5 levels between 100 m and 200 m for outer domain only). The 3-D unstructured mesh in both domains consists 2,599,495 grid cells.

The residuals of all variables were considered to be equal or less than $O(10^{-4})$ to ensure a converged solution and thus to stop the simulation in a selected trial. The simulated concentrations at each receptor were recorded at one second time interval. For a continuous and constant release in the atmosphere, the simulated concentration-field in the domain becomes invariant after a time. One minute time-average of this invariant concentration-field at the end of a simulation in each trial is considered for evaluation with the FFT-07 observations.

4.2. Boundary conditions

Recently, Kumar et al. (2015a) discussed the use of proper inflow boundary conditions in the CFD model fluidyn-PANACHE for dispersion of pollutant in an urban area. The boundary conditions in the present numerical study are constant in time. The lateral boundaries of the domain are treated as inflow and outflow boundaries based on the direction of the mean wind with respect to the domain boundary. The top boundary is treated as an outflow boundary and a no-slip bottom boundary condition is defined at the ground surface where the velocity components are set to zero. Species concentrations are set according to the specified background concentrations. No-flux boundary condition at the ground surface is considered for the concentration filed. It was assumed that the pollutant concentration is negligible at distances far enough from the sources, so that we can impose the Dirichlet type condition for concentration field as the far-field boundary condition. The fluidyn-PANACHE includes the standard wall functions to compute the drag forces on solid walls in the turbulent boundary layer (Hanjalic, 2005), given as

$$u^+ = \begin{cases} \frac{1}{\kappa}\ln(Ey^+), & \text{for} y^+ > 11.63 \\ y^+, & \text{for} y^+ < 11.63 \end{cases} \quad (1)$$

where κ (=0.40) is the von Karman constant, $u^+ = U_p/u_*$ is the non-dimensional velocity, in which U_p is the fluid velocity parallel and relative to wall, $y^+ = \rho u_* y/\mu$ is non-dimensional wall to cell-centre distance, in which y is the cell-centre to wall distance and μ is the dynamic viscosity of fluid, and E is a function of wall roughness (Jayatilleke, 1969). The effective viscosity (μ_e) at the wall is computed by $\mu_e = \mu \max(y^+/u^+, 1)$.

The inflow profiles were based on the observed surface turbulent fluxes in the atmospheric surface layer. The surface friction velocity (u_*) and the potential temperature scale (θ_*) are computed using the eddy-covariance technique with the available fast response observations from sonic anemometers in the FFT-07 field experiment. The Businger-Dyer stability functions (Businger et al., 1971; Dyer, 1974) in different atmospheric stability conditions are utilized for the wind and temperature profiles. These profiles depend on the surface turbulent fluxes and a stability parameter (the Obukhov length (L)) that vary in different atmospheric stability conditions. The computed surface turbulent fluxes and the stability parameter from the available observations during the experimental releases in each trial comprise the effect of different atmospheric stability conditions. At the inflow boundary of the computational domain, velocity, temperature, and turbulence variables are specified as follows:

(a) Wind profiles

The mixing length profiles proposed by Pena et al. (2009) are utilized for inflow boundary condition of wind profiles in stable and convective atmospheric stability conditions. These profiles in different stability conditions are given as follows:

For stable conditions:

$$U(z) = \frac{u_*}{\kappa}\left[\ln\left(\frac{z}{z_0}\right) + \frac{bz}{L}\left(1 - \frac{z}{2h}\right) + \frac{\kappa z}{\lambda}\left(1 - \frac{z}{2h}\right) - \frac{z}{h}\right] \quad (2)$$

For unstable conditions:

$$U(z) = \frac{u_*}{\kappa}\left[\ln\left(\frac{z}{z_0}\right) - \psi_m + \frac{\kappa z}{\lambda}\left(1 - \frac{z}{2h}\right) - \frac{z}{h}\right] \quad (3)$$

where b (=4.7) is an empirical constant (Businger et al., 1971; Dyer, 1974), z is the height above the ground surface, h is the height of the atmospheric boundary layer, and ψ_m is the stability correction function for momentum $\phi_m = (1 - 15z/L)^{-1/4}$ in unstable conditions by the Businger-Dyer flux-profile relationships (Businger et al., 1971; Dyer, 1974) and given as (Paulson, 1970)

$$\psi(\zeta) = \ln\left(\frac{1+x^2}{2}\right) + 2\ln\left(\frac{1+x}{2}\right) - 2\tan^{-1}(x) + \frac{\pi}{2} \tag{4}$$

in which $\zeta = z/L$ is the stability parameter and $x = (1 - 15\zeta)^{1/4}$. Here, $\lambda = 0.00027G/f$, where G is the geostrophic wind magnitude and the wind profile includes the effect of the ABL height.

(b) Temperature profiles

Logarithmic potential temperature profiles (θ) based on the Monin-Obukhov similarity theory are used to describe its vertical variation in neutral, stable, and convective conditions. These profiles are given by

$$\theta(z) = \theta_0 + \frac{\theta_*}{\kappa}\left[\ln\left(\frac{z}{z_0}\right) - \psi_h(\zeta) + \psi_h(\zeta_0)\right] \tag{5}$$

in which $\zeta_0 = z_0/L$, θ_0 is the surface potential temperature, and the stability correction functions for heat (ψ_h) in stable and unstable conditions are given as follows (Businger et al., 1971):

$$\psi(\zeta) = \begin{cases} (1-Pr_t)\ln(\zeta) - \beta_h\zeta, & \text{stable} \\ \ln(\zeta) - Pr_t \ln\left[\frac{\delta-1}{\delta+1}\right], & \text{unstable} \end{cases} \tag{6}$$

where $\delta = \sqrt{1-\gamma_h\zeta}$, in which $\beta_h = 7.8$, $\gamma_h = 11.6$, and $\mathrm{Pr}_t = 0.95$ is the turbulent Prandtl number (Högström, 1988).

(c) Prognostic turbulence profiles

The vertical profiles of the turbulent kinetic energy (k) and its dissipation rate (ϵ) are required for the proper inflow boundary conditions in the k-ϵ turbulence model. In this study, numerical solution of the one-dimensional (1-D) k-ϵ prognostic turbulence model is used for vertical profiles of k and ϵ in inflow boundary condition (Ye, 1998). These prognostic profiles were derived from the following 1-D transport equations for k and ϵ, simplified with the assumptions: (i) constant density (ρ), (ii) steady flow, (iii) neglecting convection, and (iv) neglecting horizontal gradients of all quantities:

$$\frac{\partial}{\partial z}\left(\mu + \frac{\mu_t}{\sigma_k}\right)\frac{\partial k}{\partial z} + P_k + P_b - \rho\epsilon = 0 \tag{7}$$

$$\frac{\partial}{\partial z}\left(\mu + \frac{\mu_t}{\sigma_\epsilon}\right)\frac{\partial \epsilon}{\partial z} + \frac{\epsilon}{k}[C_{\epsilon 1}(P_k + C_{\epsilon 3}P_b) - C_{\epsilon 2}\rho\epsilon] = 0 \tag{8}$$

where σ_k and σ_ϵ are respectively the Prandtl numbers for turbulent diffusion of k and ϵ, and, $C_{\epsilon 1}$, $C_{\epsilon 2}$ and $C_{\epsilon 3}$ are the empirical constants. The shear stress-related production of turbulent kinetic energy (P_k), buoyancy-related production of turbulent kinetic energy (P_b), and the turbulent eddy viscosity (μ_t) in Eqs. (7) & (8) are given by

$$P_k = \mu_t\left(\frac{\partial U}{\partial z}\right)^2, \quad P_b = \beta\frac{\mu_t}{Pr_t}g\frac{\partial \theta}{\partial z}, \quad \text{and} \quad \mu_t = \rho C_\mu \frac{k^2}{\epsilon} \tag{9}$$

where β is the coefficient of thermal expansion, g is the gravitational acceleration. The constants in the k-ϵ turbulence model (Eqs. (7)–(8)) are given as $C_{\epsilon 1} = 1.44$, $C_{\epsilon 2} = 1.92$, $C_{\epsilon 3} = -0.4$, $C_\mu = 0.09$, $\sigma_k = 1.0$, and $\sigma_\epsilon = 1.3$. $C_{\epsilon 3}$ does not play a role as buoyancy production in neutral stability conditions and therefore, it sets to zero. $C_{\epsilon 3}$ is set to -0.4 in stable condition (Peters and Baumert, 2007). For the selected vertical profiles for wind and potential temperature (Eqs. (2)–(6)), Eqs. (7) & (8) are solved using a conjugate gradient method.

5. Methods for the model performance evaluation

The performance of the CFD model is evaluated by computing the statistical performance measures between the observed and simulated concentrations for each selected trial of the FFT-07 field experiment. The computed statistical performance measures, scatter plots, quantile-quantile (Q-Q) plots provides both qualitatively and quantitatively evaluation of the CFD model's performance. The paired simulated and observed concentrations are plotted against each other in a scatter plot and it can be easily visualized the CFD model's over- or under-predictions with respect to the observations. The Q-Q plot begins with the same paired data as the scatter plots, but removes the pairing and instead ranks each of the observed and predicted data separately from lowest to highest (Chang and Hanna, 2004). A Q-Q plot is often useful to find out whether a model can generate a concentration distribution that is similar to the observed distribution.

Chang and Hanna (2004) provided a detailed analysis of the standard statistical measures for air quality model's performance evaluation. Accordingly, the standard statistical measures such as, Normalized Mean Square Error (NMSE), Fractional Bias (FB), Correlation coefficient (COR), Factor of Two (FAC2), and Index of Agreement (IA) are computed to evaluate the CFD model performance. The positive or negative values of the FB respectively indicate an overall under- or over-prediction from the observations. The NMSE characterizes the scattering in a sample. The ideal values of NMSE = 0 and FB = 0; and COR = 1, FAC2 = 1, and IA = 1 for a prefect model (Chang and Hanna, 2004). However, NMSE < 4, $-0.3 < FB < 0.3$, and FAC2 > 0.5 were the suggested bounds of these measures for an acceptable model performance by Chang and Hanna (2004). In computations of the statistical performances measures, the simulated and observed concentrations values which are smaller than the detection limit of the sensors are replaced with the detection threshold value. If both observed and predicted concentrations in a sample were below the detection limit, that sample point was removed and thus, the statistical measures were computed if both concentrations values in a pair of simulated and observed concentrations are greater than the threshold value. The sampling calibration range of the detectors used in the FFT-07 experiment was 0.025–1000 ppmv (Storwold, 2007; Yee, 2012).

6. Results and discussions

Figs. 2 & 3 show the scatter and Q-Q plots between the observed and CFD model predicted concentrations for each selected trial of the FFT-07 experiment. The computed statistical performance measures for each trial are given in Table 1. The scatter plots and statistical measures show that the CFD model's simulated concentrations are in good agreement with the observations in each trial. The scatter plots exhibit that most of the concentrations points are close to one-to-one line in each trial. The Q-Q plots in Figs. 2 (b) & 3(b) show a comparison of the predicted and observed concentrations distributions in each selected FFT-07 trial. Most of the concentration points in these Q-Q plots are roughly along the one-to-one line and it shows the comparable distributions of the simulated and observed concentrations in most of the selected FFT-07 trials. In most of the trials, the higher concentrations in Q-Q plots are more close to one-to-one line than the lower concentrations. However, in some trials, e.g., 13, 30, the distribution of the predicted concentrations are not similar to that observed as it is away from the one-to-one line, especially for the lower concentrations at far away from the source in a homogeneous terrain.

The values of NMSE are smaller than the acceptable upper bound (NMSE < 4) in all the selected trials and small values of the NMSE are observed in most of the trials (Table 1). Minimum value of NMSE (=0.16) is observed in trials 45 and 54. As one can see in the scatter plots (Fig. 2) and the extent magnitudes of NMSE (Table 1) in trials 13 and 30, larger scatteredness in these trials was observed in comparison to the other trials. In most of the trials, the simulated concentrations from the CFD model fluidyn-PANACHE under-predict from the observations (Figs. 2 & 3) and this under-prediction can easily be quantified with the positive values of FB in most of the trials (Table 1). A slightly over-prediction (FB = −0.07) was observed in trial 54 (Table 1). The simulated concentrations have good one-to-one correlation with the observations and as evident with the value of IA

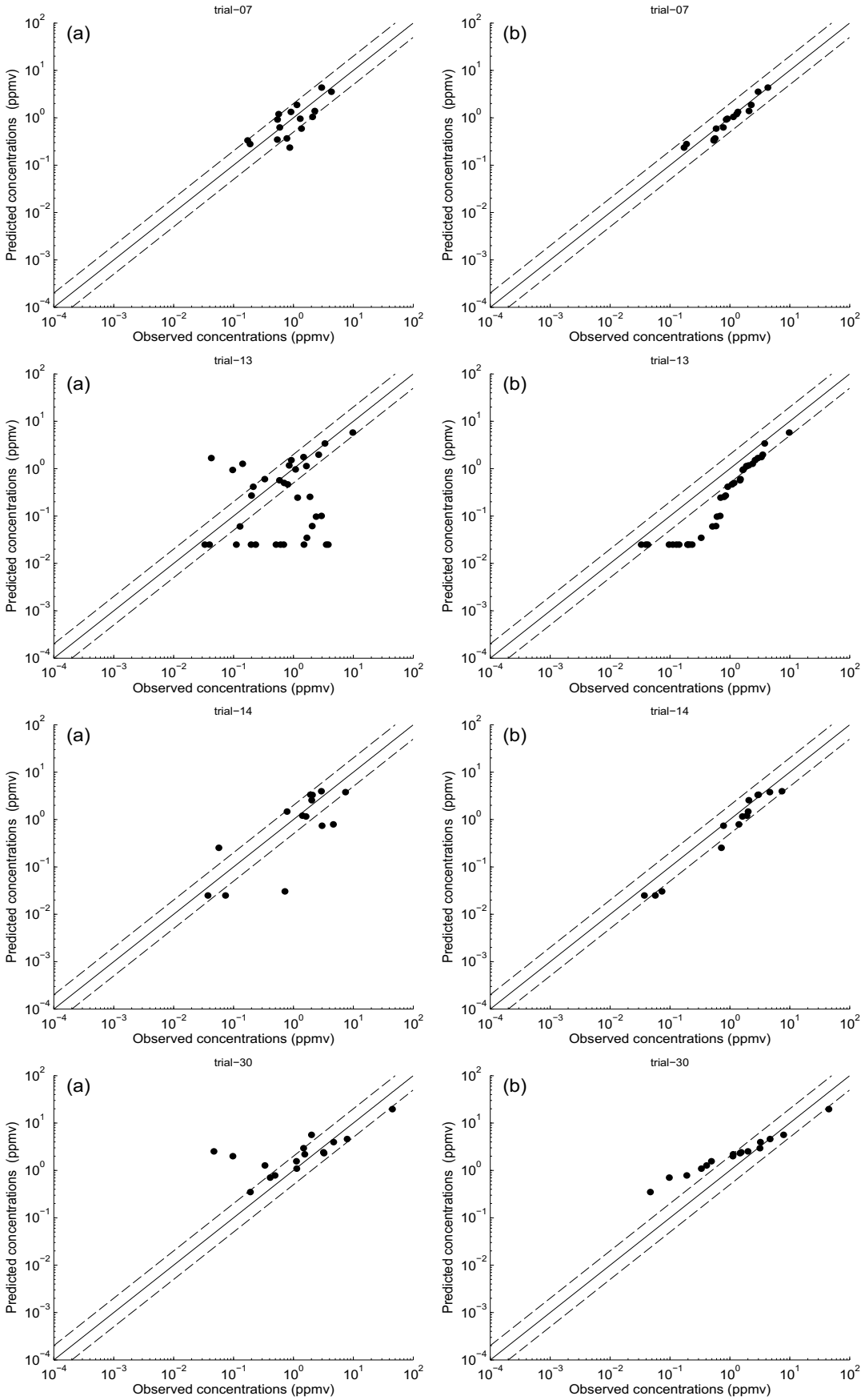

Fig. 2. (a) Scatter and (b) quantile-quantile plots between the simulated and observed concentrations for trials 07, 13, 14 & 30 in stable atmospheric conditions. The solid line is the one-to-one line and the dotted lines are factor of two lines between the observed and predicted concentrations.

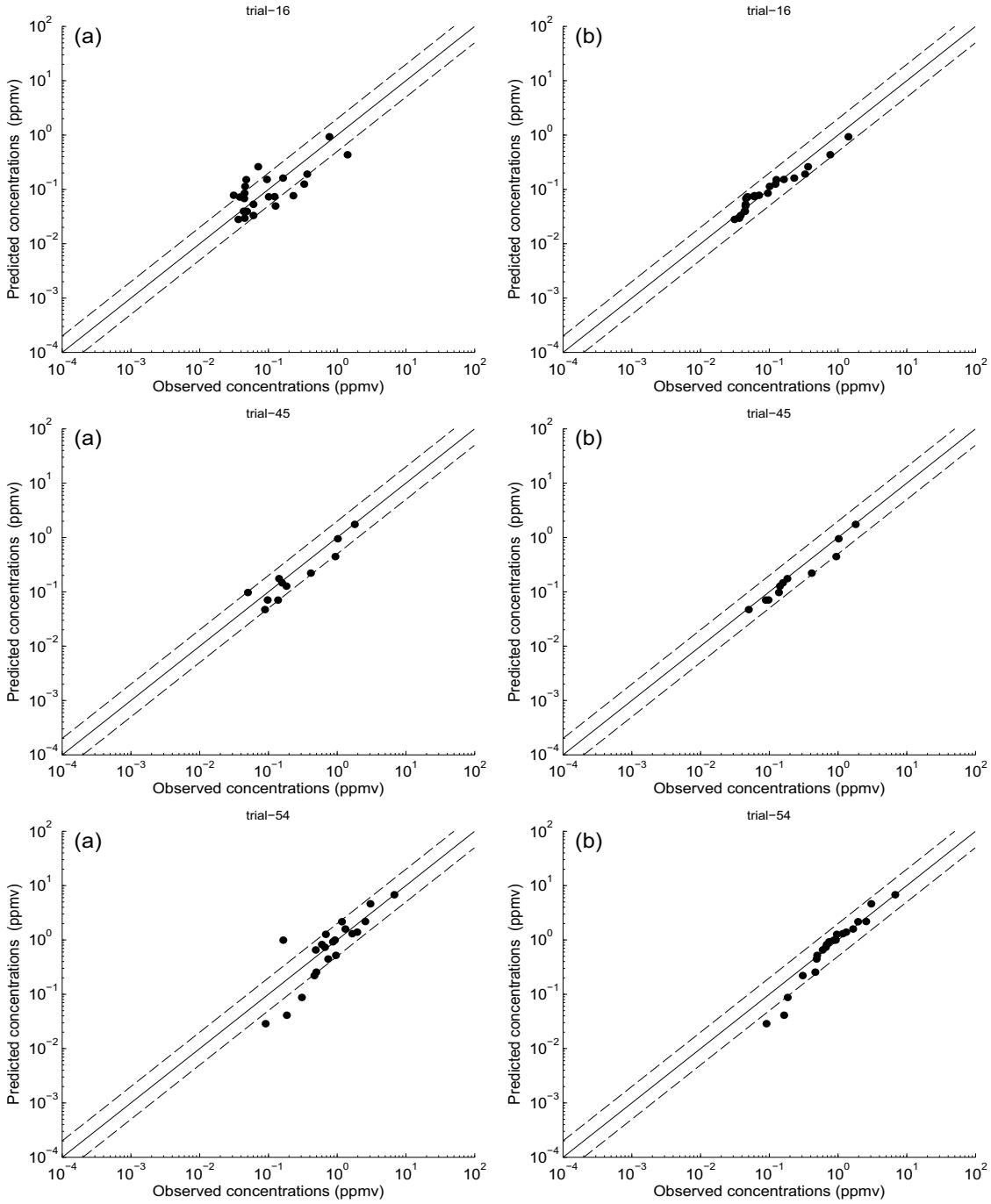

Fig. 3. (a) Scatter and (b) quantile-quantile plots between the simulated and observed concentrations for trials 16, 45, & 54 in convective atmospheric conditions. The solid line is the one-to-one line and the dotted lines are factor of two lines between the observed and predicted concentrations.

Table 1
Statistical performance measures for the each selected trial of the FFT-07 field experiment.

Trial no.	NMSE	FB	COR	FAC2 (%)	IA
07	0.28	0.06	0.83	75.0	0.91
13	2.14	0.63	0.68	45.7	0.76
14	0.84	0.24	0.58	64.3	0.73
16	1.86	0.27	0.71	65.2	0.77
30	2.76	0.30	0.97	68.8	0.81
45	0.16	0.21	0.96	90.9	0.97
54	0.16	− 0.07	0.95	76.2	0.97

(≥ 0.73) in Table 1, the CFD model's predicted concentrations have good agreement with the observed concentrations in each FFT-07 trial. The CFD model predicts maximum 90.9% of concentration points within a factor of two to the observations in trial 45 and minimum 45.7% in trial 13. In most of the trials (except in trial 13), the predicted factor of two concentration points to the observations are more than the acceptable bound 50% (Table 1). It is also visible from the scatter plots in each trial (Figs. 2 (a) & 3(a)) that the higher concentrations close to the source are in good agreement with the higher observed concentrations.

As pointed out before that in some trials, e.g., 13, the CFD code performance is not as satisfactory as observed in other trials and this may be mostly due to the large variability in the ambient wind patterns

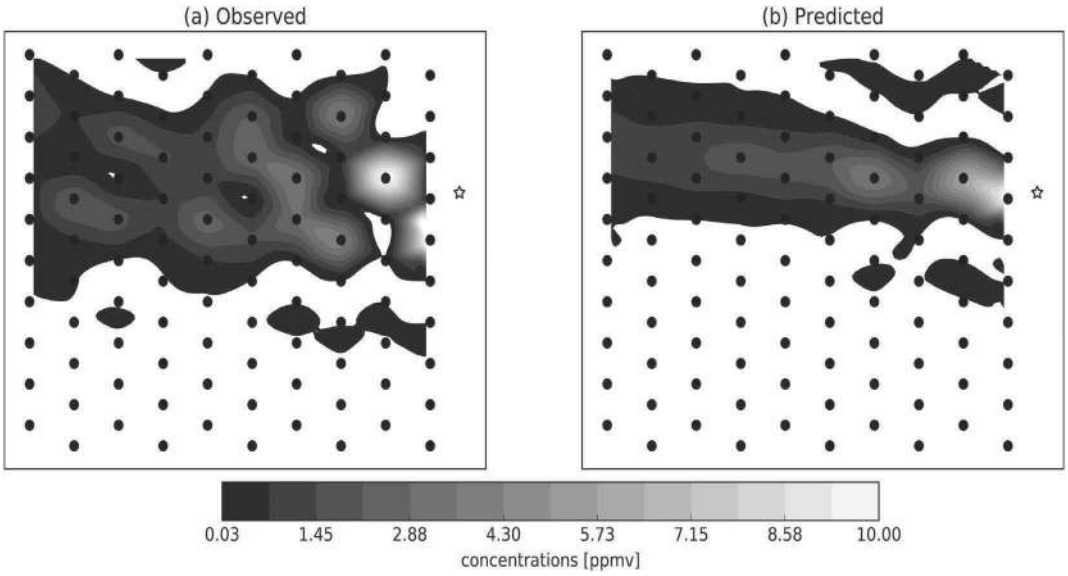

Fig. 4. (a) Observed and (b) predicted concentrations in trial 13 of the FFT-07 field experiment. In these contours, the concentrations were interpolated from their values on the receptor's locations to the grid points. The star indicates the location of source in this trial.

during the experimental release. The wind direction variability is observed large in this trial and consequently the multiple concentrations peaks are observed. Fig. 4 (a) & (b) shows the isopleths of the observed and the fluidyn-PANAACHE simulated averaged concentrations in trial 13 of the FFT-07 experiment. In order to plot the contours, the observed concentrations were interpolated from their values on the receptor's locations to other grid points in the domain. Similarly, for an equivalent comparative visualization with the observations, the contours of the predicted concentrations are also drawn from the simulated values on the receptor's locations only. Fig. 4 (b) shows only single peak of the predicted concentrations in direction of the mean wind, which is obvious as the RANS CFD simulation was performed by considering only one mean wind direction throughout the experiment release. However, two peak values of the averaged observed concentrations at different locations in different directions can easily be visualized from Fig. 4 (a). This behavior of the concentrations can not be simulated by considering the invariant wind direction and speed in the inflow boundary conditions throughout a CFD simulation. The unsteady nature of the wind boundary conditions can affect the dispersion results. Inclusion of the variation of the ambient wind conditions with time is necessary in these dispersion scenarios and the unsteady RANS (URANS) simulations instead of the RANS is required for atmospheric dispersion studies, especially when the variability in the wind is significant during the release. Thus, the URANS CFD solution can be explored in a further study for these dispersion scenarios with significant variability in the wind pattern.

Table 3 presents the ratio of the corresponding predicted concentrations to the observed peak concentrations in each selected trial of the FFT-07 field experiment. It can easily conclude from these ratios of the peak concentrations that in most of the trials, the peak concentrations are predicted within a factor of two to the observations. The factor of two ratios of these peak concentrations in unstable atmospheric conditions are two in three trials and three in four trials in stable stability conditions. However, an overall under-prediction of the predicted peak concentrations from the observed peak concentrations is observed in all considered FFT-07 trials.

6.1. Overall performance

The overall performance of the CFD model is analyzed by computing the statistical measures with the predicted and observed concentrations combined from all seven FFT-07 trials. Table 2 shows the computed statistical measures from all combined trials. Fig. 5 (a) & (b) shows the scatter and Q-Q plots between the observed and predicted concentrations from all the combined trials. These figures and the computed statistical performance measures show a good overall agreement between the CFD model's simulated and observed concentrations. From Q-Q plot for overall concentrations in Fig. 5 (b), it is visible that the concentration points forming a line that's roughly straight and it exhibited that both sets of the predicted and observed concentrations come from the same distribution.

Table 2
Statistical performance measures for overall, all stable, and all unstable trials of the FFT-07 field experiment.

Trials	NMSE	FB	COR	FAC2 (%)	IA
Overall	3.39	0.27	0.89	65.4	0.84
Stable	3.12	0.34	0.90	59.3	0.82
Unstable	0.31	0.01	0.95	74.6	0.97

Table 3
Ratio of the corresponding predicted concentrations to the observed peak concentrations in each selected trial of the FFT-07 field experiment.

Trials	07	13	14	16	30	45	54
Ratio	0.82	0.59	0.51	0.31	0.44	0.96	0.99

The NMSE value for all combined trials is 3.39 which is smaller than the accepted bound 4.0. However, the magnitude of the NMSE is large from its ideal value zero which exhibits more scatteredness between the predicted and observed concentrations in Fig. 5 (a). Overall 65.4% of the concentrations points are predicted within a factor of two to the observations. The positive value of FB (=0.27) shows that the CFD model's simulated concentrations has an overall under-prediction from the observed concentrations. A good one-to-one correlation (COR = 0.89) and IA = 0.84 show that the simulated concentrations have overall good agreement with the observations.

6.2. Performance in stable conditions

Based on the positive sign of the Obukhov length (L), it was observed that the releases in four trials 07, 13, 14, & 30 were conducted in stable atmospheric conditions. In order to evaluate the performance of

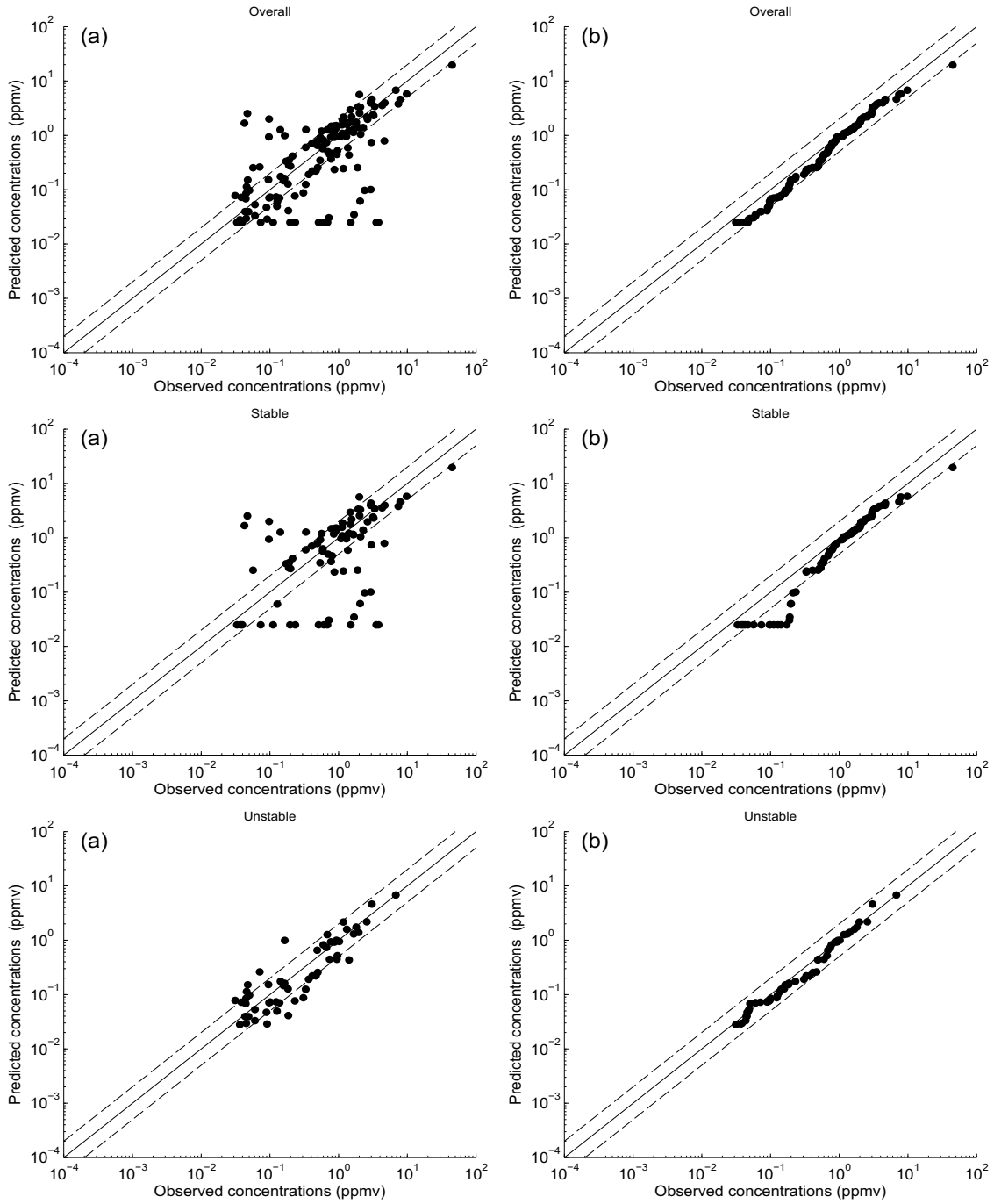

Fig. 5. (a) Scatter and (b) quantile-quantile plots between the simulated and observed concentrations for overall, all stable, and all unstable trials. The solid line is the one-to-one line and the dotted lines are factor of two lines between the observed and predicted concentrations.

the CFD model fluidyn-PANACHE in stable conditions, the statistical performance measures were separately computed for the combined data of the simulated and observed concentrations from these four trials only. The scatter and Q-Q plots for all these trials in stable atmosphere are shown in Fig. 5 (a) & (b) and Table 2 presents the corresponding statistical performance measures. These plots show that the simulated concentrations from the CFD model in stable atmospheric conditions have satisfactory agreement with the observations. This fact is also exhibited from the computed statistical performance measures in stable stability conditions. In stable conditions, the CFD model predicts 59.3% of concentrations points within a factor of two to the observations (Table 2). The NMSE (=3.12) is also within the acceptable bound for the air quality model; however, it is large in comparison to its ideal value zero. The large value of NMSE for all stable trials is due to the larger scatter observed in trials 13 & 30 (Table 1). As mentioned before, it may be due to the large variability in wind directions in these trials that was not accounted in RANS solutions by considering the invariant inflow conditions. The CFD model under-predicts from the observed concentrations (FB = 0.34). The predicted concentrations have a good one-to-one correlation (COR = 0.90) with the observations. The higher and middle concentrations in these trials are well predicted by the CFD model fluidyn-PANACHE (Fig. 5 (a)). However, a more scatter is observed for the lower concentrations at the receptors far away from the source (Fig. 5 (a)). The higher concentrations points in the Q-Q plot in Fig. 5 (b) also exhibits a similar trend of the concentration distribution in stable atmospheric conditions.

It was also observed that in stable conditions, the CFD code performance is not as satisfactory as in unstable conditions and this may be mostly due to a large variability of the ambient wind patterns during the release in these conditions. However, in stable conditions also, most of the statistical performance measures are also within the bounds for an acceptable model performance given by Chang and Hanna (2004). Due to the significant variability in the wind patterns during the experimental campaign, the URANS solution is a necessity in further studies to simulate the dispersion phenomena in these types of variable meteorological conditions with time.

6.3. Performance in unstable conditions

The Obukhov length in the remaining trials 16, 45, & 54 are observed to be negative and consequently the tracer experiments in these trials were conducted in convective atmospheric conditions. Fig. 5 (a) & (b) shows the scatter and Q-Q plots between the predicted and observed concentrations combined from these trials in unstable stability conditions. The scatter plot shows that the simulated concentrations from the CFD model in convective conditions are in good agreement with the observations. Most of the concentrations points are close to one-to-one line and the Q-Q plot in Fig. 5 (b) also exhibits the similar trend of the concentrations.

Table 2 shows the statistical performance measures for the concentrations in these combined trials in convective stability conditions. A small value of the NMSE (= 0.31) shows that a small scatter is observed between the simulated and observed concentrations. The CFD model predicts 74.6% of the concentration points within a factor of two to the observations. The predicted concentrations are slightly under-predicted (FB = 0.01) from the observations. A good one-to-one correlation (COR = 0.95) and index of agreement (IA = 0.97) is observed between the predicted and observed concentrations from all these trials in convective conditions.

It is also observed that in comparison to the stable stability, the CFD model has good agreement of the predicted concentrations with the observations in convective stability conditions (Tables 1 & 2, Figs. 2, 3, & 5). The NMSE (= 0.31) in convective conditions is smaller than that obtained in stable atmospheric stability (NMSE = 3.12) and consequently a smaller scatter between the predicted and observed concentration is observed in unstable conditions. The CFD model predicts more number of concentrations points within a factor of two to the observations in convective conditions (FAC2 = 74.6%) in comparison to the FAC2 = 59.3% in stable stability. Compared to the stable conditions, it is also observed that the predicted concentrations in unstable atmospheric conditions have better correlation and agreement with the observed concentrations.

7. Conclusions

In this study, three-dimensional CFD simulations were performed for the short-range plume dispersion in seven trials of the single continuous point release from the FFT-07 tracer field experiment in homogeneous terrain. The atmospheric conditions in these FFT-07 trials were observed in both stable and convective stability conditions. A CFD model fluidyn-PANACHE is utilized and evaluated for the near-field forward dispersion in these seven FFT-07 trials in various atmospheric stability conditions. The statistical performance measures were computed to evaluate the CFD model performance in (a) each trial separately, (b) all combined trials, (c) stable conditions only, and (d) convective stability conditions only. A comprehensive statistical analysis of the CFD model simulated concentrations is performed both qualitatively and quantitatively following various statistical performance measures.

It was observed that the simulated concentrations from the CFD model fluidyn-PANACHE are in good agreement with the observations in both stable and convective atmospheric conditions. The CFD model predicts 65.4% of the overall concentrations points within a factor of two to the observations. An overall under-prediction of the predicted concentrations is observed from the CFD simulations. It was observed that the CFD model is predicting better in convective stability conditions in comparison to the trials conducted in stable stability and this may be mostly due to a large variability in the ambient wind patterns during the experimental release in these stable conditions. In convective conditions, the CFD model predicts 74.6% of points within a factor of two to the observations which are higher than the 59.3% concentration points predicted within a factor of two in all selected trials in stable atmospheric conditions. The large variability in the ambient wind patterns during the releases in some trials in stable atmospheric conditions affected the performance of the RANS CFD solution. Inclusion of the variability of the ambient wind conditions with time is required and the unsteady RANS simulations instead of the RANS may be useful when the variability in the wind is significant during a continuous release.

The CFD simulations and a comprehensive statistical performance analysis and comparison of the results with FFT-07 observations exhibit the practical utility of the CFD modelling for short-range atmospheric dispersion problems in various stability conditions. This study is also an essential part to utilize the CFD model fluidyn-PANACHE with an inversion approach to retrieve the location and intensity of an unknown atmospheric tracer sources in various atmospheric conditions.

Acknowledgments

The Fusion Field Trail 2007 (FFT-07) database is available at https://fft07-dpg.dpg.army.mil/. The authors would like to thank the Defense Threat Reduction Agency (DTRA) for providing access to the FFT07 field experiment dataset. A sincere thanks to Nathan Platt for helping to obtain the FFT-07 dataset. The authors gratefully acknowledge Fluidyn France for use of the CFD model fluidyn-PANACHE. This work was partially supported by the RAPID project DISCARD (no. 132906009), France.

References

Bocquet, M.M., 2005. Reconstruction of an atmospheric tracer source using the principle of maximum entropy. I: theory. Q. J. R. Meteorol. Soc. 131 (610), 2191–2208. http://dx.doi.org/10.1256/qj.04.67.

Businger, J.A.J.A., Wyngaard, J.C.J.C., Izumi, Y.Y., Bradley, E.F.E.F., 1971. Flux-profile relationships in the atmospheric surface layer. J. Atmos. Sci. 28 (2), 181–189. http://dx.doi.org/10.1175/1520-0469(1971)028¡0181:FPRITA¿2.0.CO;2.

Chang, J.C.J.C., Hanna, S.R.S.R., 2004. Air quality model performance evaluation. Meteorog. Atmos. Phys. 87 (1–3), 167–196. http://dx.doi.org/10.1007/s00703-003-0070-7.

Cimorelli, A.J.A.J., Perry, S.G.S.G., Venkatram, A.A., Weil, J.C.J.C., Paine, R.R., Wilson, R.B.R.B., Lee, R.F.R.F., Peters, W.D.W.D., Brode, R.W.R.W., 2005. Aermod: a dispersion model for industrial source applications. Part I: general model formulation and boundary layer characterization. J. Appl. Meteorol. 44 (5), 682–693. http://dx.doi.org/10.1175/JAM2227.1.

Dyer, A.A., 1974. A review of flux-profile relationships. Bound.-Layer Meteorol. 7 (3), 363–372. http://dx.doi.org/10.1007/BF00240838.

Ferziger, J.H.J.H., Peric, M.M., 2002. Computational Methods for Fluid Dynamics. Springer Berlin Heidelberg.

Fluidyn-PANACHE, 2010. User Manual. FLUIDYN France/TRANSOFT International version 4.0.7 edition.

Hanjalic, K.K., 2005. Turbulence and transport phenomena: modelling and simulation. In: Turbulence Modeling and Simulation (TMS) Workshop. Technische Universitt Darmstadt.

Hanna, S.R.S.R., Paine, R.J.R.J., 1989. Hybrid plume dispersion model (HPDM) development and evaluation. J. Appl. Meteorol. 28 (3), 206–224. http://dx.doi.org/10.1175/1520-0450(1989)028¡0206:HPDMDA¿2.0.CO;2.

Högström, U.L.F.U.L.F., 1988. Non-dimensional Wind and Temperature Profiles in the Atmospheric Surface Layer: A Re-evaluation. Springer Netherlands, Dordrecht, pp. 55–78. http://dx.doi.org/10.1007/978-94-009-2935-7_6.

Jayatilleke, C.V.C.V., 1969. The influence of Prandtl number and roughness on the resistance of the laminar sublayer to momentum and heat transfer. Prog. Heat Mass Tran. 1, 193–329.

Kumar, P.P., Feiz, A.-A.A.-A., 2016. Performance analysis of an air quality CFD model in complex environments: numerical simulation and experimental validation with EMU observations. Build. Environ. 108, 30–46. http://www.sciencedirect.com/science/article/pii/S0360132316303080.

Kumar, P.P., Feiz, A.-A.A.-A., Ngae, P.P., Singh, S.K.S.K., Issartel, J.-P.J.-P., 2015a. CFD simulation of short-range plume dispersion from a point release in an urban like environment. Atmos. Environ. 122, 645–656. http://www.sciencedirect.com/science/article/pii/S1352231015304465.

Kumar, P.P., Feiz, A.-A.A.-A., Singh, S.K.S.K., Ngae, P.P., Turbelin, G.G., 2015b. Reconstruction of an atmospheric tracer source in an urban-like environment. J. Geophys. Res. Atmos. 120 (24), 12589–12604. http://dx.doi.org/10.1002/2015JD024110.

Kumar, P.P., Sharan, M.M., 2010. An analytical model for dispersion of pollutants from a continuous source in the atmospheric boundary layer. Proc. R. Soc. London A Math. Phys. Eng. Sci. 466 (2114), 383–406. http://rspa.royalsocietypublishing.org/content/466/2114/383.abstract.

Kumar, P.P., Singh, S.K.S.K., Feiz, A.-A.A.-A., Ngae, P.P., 2016. An urban scale inverse modelling for retrieving unknown elevated emissions with building-resolving simulations. Atmos. Environ. 140, 135–146. http://www.sciencedirect.com/science/article/pii/S1352231016303983.

Liu, C.-H.C.-H., Wong, C.C.C.C., 2014. On the pollutant removal, dispersion, and entrainment over two-dimensional idealized street canyons. Atmos. Res. 135–136, 128–142. http://www.sciencedirect.com/science/article/pii/S0169809513002226.

Mazzoldi, A.A., Hill, T.T., Colls, J.J.J.J., 2008. CFD and Gaussian atmospheric dispersion models: a comparison for leak from carbon dioxide transportation and storage facilities. Atmos. Environ. 42 (34), 8046–8054. http://www.sciencedirect.com/science/article/pii/S1352231008006080.

Moreira, D.D., Vilhena, M.M., Buske, D.D., Tirabassi, T.T., 2009. The state-of-art of the GILTT method to simulate pollutant dispersion in the atmosphere. Atmos. Res. 92 (1), 1–17. http://www.sciencedirect.com/science/article/pii/S0169809508001609.

Pandey, G.G., Sharan, M.M., 2015. Simulation of plume dispersion of multiple releases in Fusion Field Trial-07 experiment. Atmos. Environ. 122, 672–685. http://www.sciencedirect.com/science/article/pii/S1352231015304532.

Paulson, C.A.C.A., 1970. The mathematical representation of wind speed and temperature profiles in the unstable atmospheric surface layer. J. Appl. Meteorol. 9 (6), 857–861. http://dx.doi.org/10.1175/1520-0450(1970)009¡0857:TMROWS¿2.0.CO;2.

Pena, D.A.D.A., Gryning, S.-E.S.-E., Hasager, C.B.C.B., Courtney, M.M., 2009. Extending the wind profile much higher than the surface. In: European Wind Energy Conference and Exhibition, France, pp. 8.

Peters, H.H., Baumert, H.Z.H.Z., 2007. Validating a turbulence closure against estuarine microstructure measurements. Ocean Model. 19 (34), 183–203. http://www.sciencedirect.com/science/article/pii/S146350030700100X.

Platt, N.N., Warner, S.S., Nunes, S.M.S.M., 2008. Evaluation plan for comparative investigation of source term estimation algorithms using FUSION field trial 2007 data. Hrvatski Meteorološki Časopis 43 (43/1), 224–229.

Pudykiewicz, J.A.J.A., 1998. Application of adjoint tracer transport equations for evaluating source parameters. Atmos. Environ. 32 (17), 3039–3050. http://www.sciencedirect.com/science/article/pii/S1352231097004809.

Sharan, M.M., Issartel, J.-P.J.-P., Singh, S.K.S.K., Kumar, P.P., 2009. An inversion technique for the retrieval of single-point emissions from atmospheric concentration measurements. Proc. R. Soc. London A Math. Phys. Eng. Sci. 465, 2069–2088. http://rspa.royalsocietypublishing.org/content/early/2009/04/09/rspa.2008.0402.abstract.

Sharan, M.M., Yadav, A.K.A.K., Singh, M.M., Agarwal, P.P., Nigam, S.S., 1996. A mathematical model for the dispersion of air pollutants in low wind conditions. Atmos. Environ. 30 (8), 1209–1220. http://www.sciencedirect.com/science/article/pii/1352231095004424.

Singh, S.K.S.K., Sharan, M.M., 2013. Simulation of plume dispersion from single release in Fusion Field Trial-07 experiment. Atmos. Environ. 80, 50–57. http://www.sciencedirect.com/science/article/pii/S135223101300602X.

Stein, A.F.A.F., Draxler, R.R.R.R., Rolph, G.D.G.D., Stunder, B.J.B.B.J.B., Cohen, M.D.M.D., Ngan, F.F., 2015. NOAA's HYSPLIT atmospheric transport and dispersion modeling system. Bull. Am. Meteorol. Soc. 96 (12), 2059–2077.

Stohl, A.A., Forster, C.C., Frank, A.A., Seibert, P.P., Wotawa, G.G., 2005. Technical note: the Lagrangian particle dispersion model flexpart version 6.2. Atmos. Chem. Phys. 5 (9), 2461–2474. http://www.atmos-chem-phys.net/5/2461/2005/.

Storwold, D.P.D.P., 2007. Detailed Test Plan for the Fusing Sensor Information From Observing Networks (FUSION) Field Trial 2007 (FFT 07), West Desert Test Center. US Army Dugway Proving Ground WDTC Document No. WDTC-TP-07-078.

Vilhena, M.M., Costa, C.C., Moreira, D.D., Tirabassi, T.T., 2008. A semi-analytical solution for the three-dimensional advection–diffusion equation considering non-local turbulence closure. Atmos. Res. 90 (1), 63–69. http://www.sciencedirect.com/science/article/pii/S0169809508000914.

Ye, L.L., 1998. Numerical Evaluation of Wind-induced Dispersion of Pollutants Around Buildings. Concordia University Ph.D. Thesis.

Yee, E.E., 2012. Inverse dispersion for an unknown number of sources: model selection and uncertainty analysis. ISRN Appl. Math. 2012.

Zhang, Z.Z., Chen, Q.Q., 2007. Comparison of the Eulerian and Lagrangian methods for predicting particle transport in enclosed spaces. Atmos. Environ. 41 (25), 5236–5248. http://www.sciencedirect.com/science/article/pii/S1352231007002786.